

Adsorption of Small Molecules in LTA Zeolites. 1. NH<sub>3</sub>, CO<sub>2</sub>, and H<sub>2</sub>O in Zeolite 4A

E. Jaramillo and M. Chandross\*

Sandia National Laboratories, Albuquerque, New Mexico 87185

Received: May 4, 2004; In Final Form: August 9, 2004

We have developed force fields for the calculation of adsorption of NH<sub>3</sub>, CO<sub>2</sub>, and H<sub>2</sub>O on zeolite 4A by performing Gibbs ensemble Monte Carlo simulations to fit experimental isotherms at 298 K. The calculated NH<sub>3</sub> and CO<sub>2</sub> isotherms are in excellent agreement with experimental data over a wide range of temperatures and several orders of magnitude in pressure. We have calculated isotherms for H<sub>2</sub>O in 4A using two different models and have found that H<sub>2</sub>O saturates zeolite 4A even at pressures as low as 0.01 kPa for the range of temperatures studied. We have studied the geometry of the adsorption sites and their dependence on loading. At low pressures, CO<sub>2</sub> molecules adsorb with their longitudinal axis pointing toward the center of the supercage, whereas at higher pressures, the two oxygen atoms are equidistant from the Na atom in the binding site.

## I. Introduction

Zeolites from the LTA family (3A, 4A, and 5A, where the *n* in *n*A refers to the pore size in Å) are commonly used as industrial desiccants. Although the ubiquitous silica gel desiccants perform adequately for general use, their amorphous structure leads to the adsorption of a large number of molecules in addition to water. The LTA zeolites, however, exhibit strong preferential adsorption of water because of their small pore openings as well as the polar nature of the zeolite cage itself. This affinity for water makes these zeolites ideal desiccants for applications in which moisture control is crucial, such as the packaging of sealed electronics. The presence of water in electronic assemblies can lead to corrosion, conduction through dendritic growth, and even conduction through the water itself if large quantities are present.

In addition to water, however, the LTA zeolites adsorb a number of small molecules including O<sub>2</sub>, N<sub>2</sub>, NH<sub>3</sub>, CO<sub>2</sub>, and others. It is therefore a concern that reactions among adsorbed molecules, such as  $\text{NH}_3 + \text{CO}_2 + \text{H}_2\text{O} \rightarrow \text{NH}_4^+ + \text{HCO}_3^-$ , may occur within the zeolite, leading to a reduction in water capacity. For example, given the reaction above, cation exchange of NH<sub>4</sub><sup>+</sup> with the sodium cations of the LTA zeolites could lead to blocking of the pores and eventually the failure of the desiccant to adsorb water. To investigate the likelihood of such a reaction taking place, we have studied the adsorption of NH<sub>3</sub>, CO<sub>2</sub>, and H<sub>2</sub>O in zeolite 4A. Our ultimate goal is to study the multicomponent adsorption of these three compounds in zeolite 3A to determine the siting of adsorbents around possible reaction sites. However, because there is little experimental data available for adsorption in 3A we have begun our study with the more prevalent 4A and will present results on 3A in future papers.

Zeolite 4A is an aluminosilicate zeolite with a cubic unit cell of 24.555 Å on a side. (Figure 1). Each unit cell contains eight α cages or supercages of diameter 11.4 Å and eight β or sodalite cages of diameter 6.6 Å. The openings to the α cages are eight-membered oxygen rings (8MR) that are approximately 5 Å across. The presence of charge-balancing cations (Na/K for 3A, Na for 4A, and Na/Ca for 5A) reduces the effective pore size of the opening to 3 or 4 Å, depending on the type.

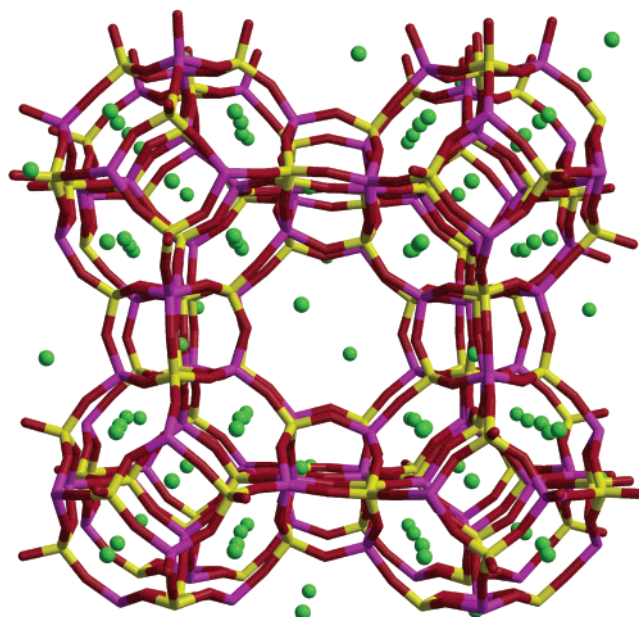


**Figure 1.** Schematic diagram of zeolite 4A with silicon atoms shown in yellow, aluminum in purple, oxygen in red, and sodium in green.

The β cages connect to the α through six-membered rings (6MR) that are too small for most molecules to pass through. The β cages are connected to each other by four-membered rings (4MR).

Other groups have reported theoretical and computational studies on water adsorption in zeolite 4A. Lee et al.<sup>1</sup> and Faux and co-workers<sup>2–4</sup> have performed MD in hydrated zeolite 4A with fixed numbers of water molecules in order to observe their diffusion and locations in the zeolite cell. Koh and Jhon<sup>5</sup> obtained the positions and differential and integral heats of sorption of water in zeolite 4A using a theoretical approach. In the only paper that reports MD of carbon dioxide in related zeolites, Mizukami et al.<sup>6</sup> studied the separation of CO<sub>2</sub> and N<sub>2</sub> using a zeolite NaY membrane. We are not aware of any computational studies of ammonia in zeolite 4A.

In the present paper, we report the development of potential parameters for CO<sub>2</sub> and NH<sub>3</sub> that are optimized for adsorption

\* Corresponding author. E-mail: mechand@sandia.gov.

**TABLE 1: Partial Charges Used in Equation 1 for the Interaction Potentials<sup>a</sup>**

atom	charge ( <i>e</i> )
O <sub>Z</sub>	-1.86875
Si	3.700
Al	2.775
Na	1.000
N	-1.020
H <sub>N</sub>	0.340
C	0.800
O <sub>C</sub>	-0.400
O <sub>W</sub> (SPC/E)	-0.8476
H <sub>W</sub> (SPC/E)	0.4238
O <sub>W</sub> (TIP3P)	-0.8340
H <sub>W</sub> (TIP3P)	0.4170

<sup>a</sup> Subscripts Z, N, C, and W refer to atoms in the zeolite, NH<sub>3</sub>, CO<sub>2</sub>, and H<sub>2</sub>O molecules, respectively.

in zeolite 4A. We present adsorption isotherms obtained by Gibbs ensemble Monte Carlo simulations for CO<sub>2</sub>, NH<sub>3</sub>, and H<sub>2</sub>O at different temperatures and identify the geometry of the adsorption sites and their dependence on loading. A comparison to available experimental data is also shown.

The remainder of this article is organized as follows. Section II outlines the details of our approach, including the new parametrization and the calculation of adsorption isotherms. Section III provides results and discussion of the force field accuracy, isotherm data, and adsorption site geometry, and section IV offers a summary of our findings as well as concluding remarks.

## II. Methodology

Here we describe a series of Gibbs ensemble Monte Carlo (GEMC) simulations of ammonia, carbon dioxide, and water in zeolite 4A to obtain the corresponding adsorption isotherms at various temperatures and to determine the geometry of the adsorption sites. In what follows, we describe the models of the zeolite and guest atoms, the potential developed, and the GEMC simulations.

**A. Zeolite and Guest Molecule Models.** Our zeolite model is identical to that used by Faux et al.<sup>2-4</sup> One unit cell of zeolite 4A contains 96 Si, 96 Al, and 384 O atoms bridging the Si and Al. Löwenstein's rule<sup>7</sup> preventing Al—O—Al linkages was enforced by alternating Si and Al tetrahedra. To balance charge, 96 Na atoms are located in the structure as follows: 64 in sites Na(1), 24 in sites Na(2), and 8 in sites Na(3) corresponding to 6MR, 8MR, and 4MR windows, respectively.<sup>2-4,8-9</sup> The GEMC method allows for the insertion of molecules throughout the zeolite without regard to the physical diffusion pathways. Molecules of both NH<sub>3</sub> and CO<sub>2</sub> are therefore placed within the β cages, even though this is unphysical. For these molecules, purely repulsive ghost atoms of zero mass and charge were placed at the center of the β cages to prevent placement inside these cages. Because water molecules can move through the 6MR window between the supercage and the β cage, ghost atoms were not used during the calculation of H<sub>2</sub>O adsorption.

**B. Zeolite and Guest Potentials.** The zeolite potential used in this work is that used by Faux and co-workers.<sup>2-4</sup> It contains two-body Coulombic, Lennard-Jones, and Buckingham terms. The form of the potential is

$$V_{ij} = \frac{q_i q_j}{r_{ij}} + A e^{-r/\rho} - C r_{ij}^{-6} + 4 \epsilon_{ij} \left[ \left( \frac{\sigma_{ij}}{r_{ij}} \right)^{12} - \left( \frac{\sigma_{ij}}{r_{ij}} \right)^6 \right]$$

The potential charges used are given in Table 1. The potential parameters employed for the calculation of NH<sub>3</sub> and CO<sub>2</sub>

**TABLE 2: Potential Parameters for NH<sub>3</sub> Isotherms**

species	$\epsilon_{ij}$ (kcal mol <sup>-1</sup> )	$\sigma_{ij}$ (Å)
O <sub>Z</sub> —N	0.208	3.230
O <sub>Z</sub> —H <sub>N</sub>	0.087	2.770
Na—N	0.082	3.310
Na—H <sub>N</sub>	0.035	2.850
N—N	0.170	3.420
N—H <sub>N</sub>	0.071	2.960
H <sub>N</sub> —H <sub>N</sub>	0.000	0.000

**TABLE 3: Potential Parameters for CO<sub>2</sub> Isotherms**

species	$\epsilon_{ij}$ (kcal mol <sup>-1</sup> )	$\sigma_{ij}$ (Å)
O <sub>Z</sub> —C	0.122	2.897
O <sub>Z</sub> —O <sub>C</sub>	0.236	3.255
Na—C	0.048	2.977
Na—O <sub>C</sub>	0.094	3.335
C—C	0.058	2.753
C—O <sub>C</sub>	0.113	3.112
O <sub>C</sub> —O <sub>C</sub>	0.219	3.470

**TABLE 4: SPC/E Potential Parameters for H<sub>2</sub>O Isotherms**

species	$\epsilon_{ij}$ (kcal mol <sup>-1</sup> )	$\sigma_{ij}$ (Å)
O <sub>Z</sub> —O <sub>W</sub>	0.560	2.495
Si—O <sub>W</sub>	0.186	1.621
Al—O <sub>W</sub>	0.118	1.692
O <sub>Z</sub> —H <sub>W</sub>	0.255	2.227
Si—H <sub>W</sub>	0.085	1.354
Al—H <sub>W</sub>	0.054	1.425
O <sub>W</sub> —O <sub>W</sub>	0.155	3.166
O <sub>W</sub> —H <sub>W</sub>	0.000	0.000
H <sub>W</sub> —H <sub>W</sub>	0.000	0.000

species	$A_{ij}$ (kcal mol <sup>-1</sup> )	$\rho_{ij}$ (Å)
Na—O <sub>W</sub>	134 941.9	0.2387

**TABLE 5: TIP3P Potential Parameters for H<sub>2</sub>O Isotherms**

species	$\epsilon_{ij}$ (kcal mol <sup>-1</sup> )	$\sigma_{ij}$ (Å)
O <sub>Z</sub> —O <sub>W</sub>	0.555	2.487
Si—O <sub>W</sub>	0.184	1.614
Al—O <sub>W</sub>	0.117	1.685
O <sub>Z</sub> —H <sub>W</sub>	0.255	2.227
Si—H <sub>W</sub>	0.085	1.354
Al—H <sub>W</sub>	0.054	1.425
O <sub>W</sub> —O <sub>W</sub>	0.152	3.151
O <sub>W</sub> —H <sub>W</sub>	0.000	0.000
H <sub>W</sub> —H <sub>W</sub>	0.000	0.000

species	$A_{ij}$ (kcal mol <sup>-1</sup> )	$\rho_{ij}$ (Å)
Na—O <sub>W</sub>	134 941.9	0.2387

isotherms were fit to the experimental adsorption isotherms at 298 K and are given in Tables 2 and 3, respectively. Two potentials have been used for water isotherms: the SPC/E potential<sup>14</sup> (Table 4) and the TIP3P potential (Table 5).<sup>15</sup> The adsorbed molecules were taken as rigid, with bond lengths of 1.010 Å for the N—H bond in NH<sub>3</sub>,<sup>16</sup> 1.143 Å for the C—O bond in CO<sub>2</sub>,<sup>17</sup> and 1.000 and 0.9572 Å for the O—H bond of H<sub>2</sub>O for the SPC/E and TIP3P potentials, respectively. The bond angles were taken as 106.4° for H—N—H,<sup>16</sup> 180.0° for O—C—O, and 109.47 and 104.52° for H—O—H for the SPC/E and TIP3P potentials, respectively.

**C. Gibbs Ensemble Monte Carlo Simulations.** All simulations were performed using the Monte Carlo for Complex Chemical Systems program (MCCCS Towhee) developed by Martin and co-workers.<sup>12</sup> The isotherms were calculated with the Gibbs ensemble Monte Carlo method, allowing guest particle moves, box volume changes, and guest particle transfers between

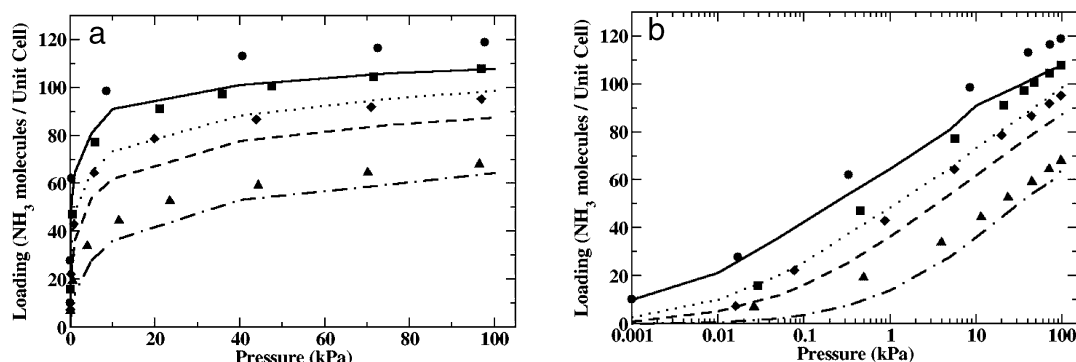


**Figure 2.** Experimental and simulated adsorption isotherms for  $\text{NH}_3$  on zeolite 4A on (a) linear and (b) logarithmic scales. Experimental isotherms from Helminen et al.<sup>10,11</sup> at 298 K (●), 323 K (■), 343 K (◆), and 393 K (▲). Simulated isotherms at 298 K (—), 323 K (···), 343 K (---), and 393 K (-.-).

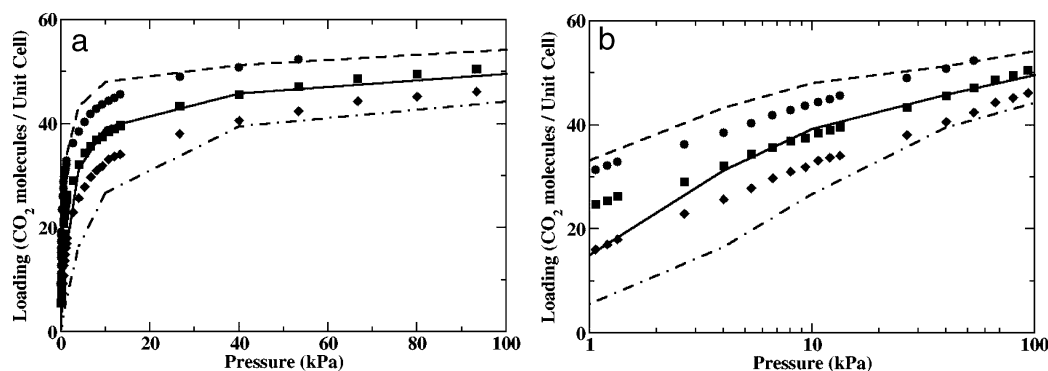


**Figure 3.** Experimental and simulated adsorption isotherms for  $\text{CO}_2$  on zeolite 4A on (a) linear and (b) logarithmic scales. Experimental isotherms from the manufacturer<sup>13</sup> at 273 K (●), 298 K (■), and 323 K (◆). Simulated isotherms at 273 K (---), 298 K (—), and 323 K (-.-).

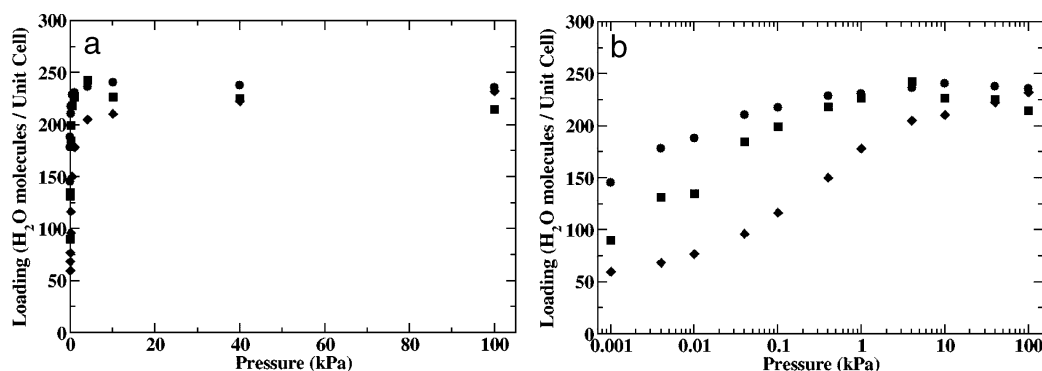


**Figure 4.** Simulated adsorption isotherms for  $\text{H}_2\text{O}$  on zeolite 4A using the SPC/E potential on (a) linear and (b) logarithmic scales at 298 K (●), 323 K (■), and 373 K (◆).

boxes. The zeolite frame and the extraframework cations were kept fixed, whereas guest molecules were taken as rigid bodies.

**D. Fitting of Parameters.** Several sets of force fields were considered for the simulation of ammonia<sup>16,18,19</sup> and carbon dioxide isotherms.<sup>17,20–26</sup> Of these, some were not optimized for the simulation of zeolite adsorption,<sup>16,26</sup> and some were used for zeolites lacking extraframework cations.<sup>17,21–23</sup> The remaining were used in the simulation of faujasites<sup>19,20,24,25</sup> and were tested in the current context but proved not to be transferable or produced distorted isotherms. The parameters used in this work were therefore inspired by parameters from the literature but were primarily obtained by trial and error, fitting them to the available experimental isotherms.

### III. Results and Discussion

**A.  $\text{NH}_3$  Adsorption Isotherms.** The potential parameters for  $\text{NH}_3$  adsorption were fit to the experimental isotherm at 298 K

and then used to calculate the isotherms at 323, 343, and 393 K. Figure 2 shows the adsorption isotherms for  $\text{NH}_3$  on zeolite 4A at different temperatures and their comparison with experimental results obtained by Helminen et al.<sup>10,11</sup> The errors in the simulations are approximately 10% of the calculated values and are not shown in the Figures. The agreement between the experimental and simulated isotherms is very good, and it is remarkable that it extends over 5 orders of magnitude in pressure and 100 K in temperature. Six different adsorption sites were identified for  $\text{NH}_3$  in zeolite 4A. Two are single-cation adsorption sites, whereas in four of them the ammonia molecule is interacting with two Na cations. The two single-cation adsorption sites, hereafter A and B, correspond to binding to a Na(1) cation and a Na(2) cation, respectively. No ammonia was detected bound to a single Na(3) cation, perhaps because the proximity of the framework atoms makes this arrangement unfavorable. The four two-cation binding sites correspond to binding to Na(1) and Na(2) cations (hereafter C), Na(1) and

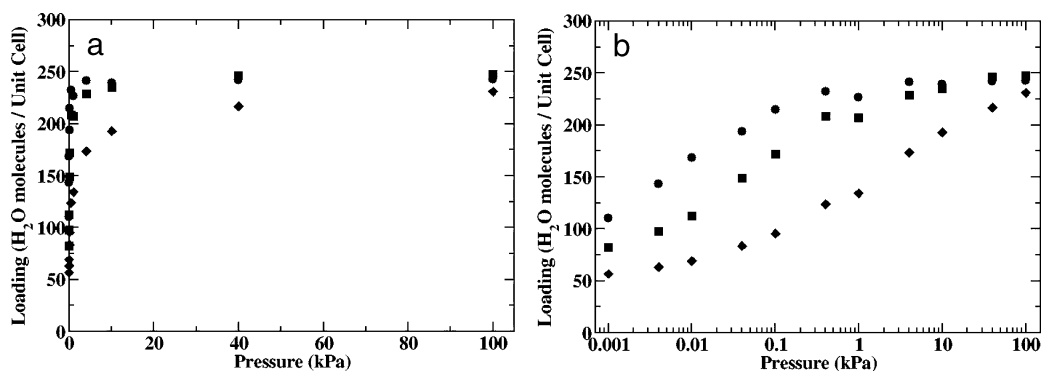


**Figure 5.** Simulated adsorption isotherms for H<sub>2</sub>O on zeolite 4A using the TIP3P potential in (a) linear and (b) logarithmic scales at 298 K (●), 323 K (■), and 373 K (◆).

**TABLE 6: Average Distances between Cations and Atoms of NH<sub>3</sub> Adsorbed in Zeolite 4A**

binding site	cation site	distance between cation and NH <sub>3</sub> atoms			
		N	H	H	H
A	Na(1)	3.61	3.18	3.69	4.54
B	Na(2)	2.92	2.70	3.43	3.79
C	Na(1)	3.56	3.54	3.47	3.82
	Na(2)	2.77	3.10	3.25	3.49
D	Na(1)	3.36	2.97	3.72	4.29
	Na(3)	3.59	4.11	3.77	4.18
E	Na(2)	2.83	2.83	3.42	3.63
	Na(2)	3.05	3.63	3.63	3.00
F	Na(2)	3.24	2.85	3.17	4.19
	Na(3)	3.05	4.03	2.98	3.14

Na(3) cations (hereafter D), two Na(2) cations (hereafter E), and Na(2) and Na(3) cations (hereafter F). Table 6 shows the average distances between cations and the atoms of ammonia molecules adsorbed in zeolite 4A. Binding sites D and F have the largest distances between the cations and the atoms of ammonia, demonstrating the avoidance of close contacts with framework atoms. The average nitrogen–nitrogen distance in a saturated zeolite 4A is 4.3 Å, which shows the close proximity of the adsorbents in the zeolite.

**B. CO<sub>2</sub> Adsorption Isotherms.** The potential parameters for CO<sub>2</sub> adsorption were fit to the experimental isotherm at 298 K and then used to calculate the isotherms at 277 and 323 K. Figure 3 shows the adsorption isotherms for CO<sub>2</sub> on zeolite 4A at different temperatures and their comparison with the experimental isotherms from the manufacturer.<sup>13</sup> The agreement between the experimental and simulated isotherms is excellent for pressures greater than 3 kPa. At lower pressures, there is a deviation of the simulated isotherms toward lower loadings. These results are also in agreement with the experimental isotherms obtained at different temperatures by Yucel and Ruthven.<sup>27</sup> Three different adsorption sites were identified for CO<sub>2</sub> in zeolite 4A. Binding site A is a single-cation site in which the CO<sub>2</sub> molecule is coordinated to a Na(1) cation. In this site, the carbon dioxide molecule has its longitudinal axis aligned in such a way that one end points toward the cation and the other points toward the center of the supercage. This is the most common site for adsorption at low pressures. Binding site B involves the coordination of the adsorbed molecule with a Na(1) cation and a Na(2) cation. Each one of the oxygens from CO<sub>2</sub> is interacting with one of the coordinating cations. In this site, the longitudinal axis of the molecule is aligned in such a way that each end points to one of the coordinating cations and the molecule is somewhat closer to the Na(1) than to the Na(2)

**TABLE 7: Average Distances between Cations and Atoms of CO<sub>2</sub> Adsorbed in Zeolite 4A**

binding site	cation site	distance between cation and CO <sub>2</sub> atoms		
		O	C	O
A	Na(1)	3.11	3.85	4.76
B	Na(1)	3.07	3.74	4.64
	Na(2)	5.15	4.14	3.21
C	Na(1)	3.27	3.83	4.62
	Na(2)	5.02	4.12	3.31
	Na(3)	4.78	4.40	3.08

cation. A carbon dioxide molecule in binding site C is coordinated to three cations, each of a different type. One end of the longitudinal axis points to the Na(1) cation, and the other points to a point between the Na(2) and Na(3) cations. The distances from each end to the nearby coordinating cations are about the same. Sites B and C are more populated at the highest pressures studied here. Table 7 shows the average distances between cations and the atoms of carbon dioxide molecules adsorbed in zeolite 4A. The average oxygen–oxygen distance between neighboring CO<sub>2</sub> molecules in a saturated zeolite 4A is 3.75 Å.

**C. H<sub>2</sub>O Adsorption Isotherms.** Two sets of potential parameters, SPC/E<sup>14</sup> and TIP3P,<sup>15</sup> were used to calculate H<sub>2</sub>O adsorption. The potentials were used as given, and no fitting was attempted because we are unaware of any experimental isotherms for comparison. Figures 4 and 5 show the H<sub>2</sub>O adsorption isotherms in zeolite 4A. The isotherms obtained using the two models are similar. Both sets of potentials provide saturation of H<sub>2</sub>O at 298 K for pressures higher than 0.1 kPa with saturation values of 235 and 243 H<sub>2</sub>O molecules/unit cell of 4A for SPC/E and TIP3P potentials, respectively. At 323 K, saturation is reached at pressures higher than 0.5 kPa, and at 373 K, saturation is reached at about 100 kPa. The saturation value obtained is slightly higher than the 224 H<sub>2</sub>O molecules/unit cell 4A given by Breck<sup>9</sup> but within the 10% error bar of our simulation method. At pressures lower than the saturation pressure at each temperature, the simulated isotherms show a consistently higher adsorption of H<sub>2</sub>O using the SPC/E potential rather than the TIP3P potential (Figure 6). At saturation, there are an average of 4.1 H<sub>2</sub>O molecules/ $\beta$  cage, which is in agreement with the simulation results of Faux et al.<sup>2</sup> (3.75 molecules/ $\beta$  cage) and the X-ray measurements of Gramlich and Meier.<sup>18</sup> Also at saturation, the average distance between an oxygen from H<sub>2</sub>O and the closest Na cation is 2.75 Å, and the average distance between two oxygen atoms from different water molecules is 2.75 Å. These results are in agreement with the findings of Faux et al.<sup>2</sup>



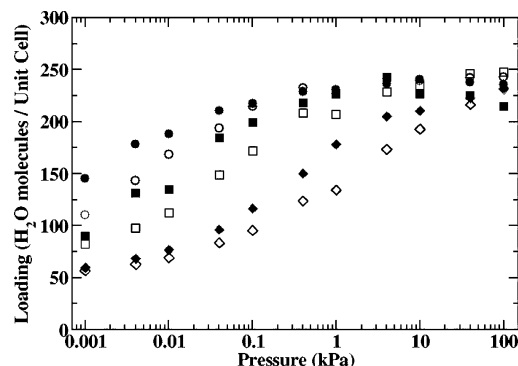


**Figure 6.** Comparison of the simulated adsorption isotherms for H<sub>2</sub>O on zeolite 4A obtained using the SPC/E (filled symbols) and TIP3P (empty symbols) potentials at 298 K (●, ○), 323 K (■, □), and 373 K (◆, ◇).

#### IV. Summary and Concluding Remarks

We have developed accurate potentials for the adsorption of NH<sub>3</sub> and CO<sub>2</sub> in zeolite 4A. We have obtained adsorption isotherms using these potentials along with existing potentials for water. There is good agreement between the simulated isotherms and the experimental ones. Our siting studies have found the preferred binding sites for NH<sub>3</sub>, CO<sub>2</sub>, and H<sub>2</sub>O at high and low pressures. Future work will involve extending our models to simulate adsorption accurately in zeolites 3A and 5A as well as studies of binary and ternary mixtures.

**Acknowledgment.** We thank David A. Faux (University of Surrey, U.K.) for providing us with the zeolite model and associated information. We thank Jarkko Helminen and Erkki Paatero (Lappeenranta University of Technology, Lappeenranta, Finland) for providing us with their experimental data on NH<sub>3</sub> isotherms. We thank Marcus Martin for assistance with the GEMC code. We thank David S. Sholl (Carnegie-Mellon University) for useful discussions. Sandia is a multiprogram laboratory operated by Sandia Corporation, a Lockheed Martin

Company, for the United States Department of Energy's National Nuclear Security Administration under contract DE-AC04-94AL85000.

#### References and Notes

- (1) Lee, S. H.; Moon, G. K.; Choi, S. G.; Kim, H. S. *J. Phys. Chem.* **1994**, *98*, 1561.
- (2) Faux, D. A.; Smith, W.; Forester, T. R. *J. Phys. Chem. B* **1997**, *101*, 1762.
- (3) Faux, D. A. *J. Phys. Chem. B* **1998**, *102*, 10658.
- (4) Faux, D. A. *J. Phys. Chem. B* **1999**, *103*, 7803.
- (5) Koh, K. O.; Jhon, M. S. *Zeolites* **1985**, *5*, 313.
- (6) Mizukami, K.; Takaba, H.; Kobayashi, Y.; Oumi, Y.; Belosludov, R. V. *J. Membr. Sci.* **2001**, *188*, 21.
- (7) Löwenstein, M. *Am. Mineral.* **1954**, *39*, 92.
- (8) Pluth, J. J.; Smith, J. V. *J. Am. Chem. Soc.* **1980**, *102*, 4704.
- (9) Breck, D. W. *Zeolite Molecular Sieves: Structure, Chemistry, and Use*; Wiley: New York, 1974.
- (10) Helminen, J.; Helenius, J.; Paatero, E.; Turunen, I. *AIChE J.* **2000**, *46*, 1541.
- (11) Helminen, J.; Helenius, J.; Paatero, E.; Turunen, I. *J. Chem. Eng. Data* **2001**, *46*, 391.
- (12) Martin, M. G.; Siepmann, J. I. *J. Phys. Chem. B* **1999**, *103*, 4508.
- (13) Davison 4A Molecular Sieves Technical Product Data. W. R. Grace & Co.: Baltimore, MD.
- (14) Berendsen, H. J. C.; Grigera, J. R.; Straatsma, T. P. *J. Phys. Chem.* **1987**, *91*, 6269.
- (15) Jorgensen, W. L.; Chandrasekhar, J.; Madura, J. D.; Impey, R. W.; Klein, M. L. *J. Chem. Phys.* **1983**, *79*, 926.
- (16) Rizzo, R. C.; Jorgensen, W. L. *J. Am. Chem. Soc.* **1999**, *121*, 4827.
- (17) Makrodimitris, K.; Papadopoulos, G. K.; Theodorou, D. N. *J. Phys. Chem. B* **2001**, *105*, 777.
- (18) Gramlich, V.; Meier, W. M. *Z. Kristallogr.* **1971**, *133*, 134.
- (19) Brändle, M.; Sauer, J. *J. Mol. Catal. A* **1997**, *119*, 19.
- (20) Kiselev, A. V.; Du, P. Q. *J. Chem. Soc., Faraday Trans. 2* **1981**, *77*, 1.
- (21) Demontis, P.; Kärger, J.; Suffritti, G. B.; Tilocca, A. *Phys. Chem. Chem. Phys.* **2000**, *2*, 1455.
- (22) Goj, A.; Sholl, D. S.; Akten, E. D.; Kohen, D. *J. Phys. Chem. B* **2002**, *106*, 8367.
- (23) Hirotsu, A.; Mizukami, K.; Miura, R.; Takaba, H.; Miya, T.; Fahmi, A.; Stirling, A.; Kubo, M.; Miyamoto, A. *Appl. Surf. Sci.* **1997**, *120*, 81.
- (24) Karavias, F.; Myers, A. L. *Mol. Simul.* **1991**, *8*, 23.
- (25) Karavias, F.; Myers, A. L. *Mol. Simul.* **1991**, *8*, 51.
- (26) Potoff, J. J.; Siepmann, J. I. *AIChE J.* **2001**, *47*, 1676.
- (27) Yucel, H.; Ruthven, D. M. *J. Colloid Interface Sci.* **1980**, *74*, 186.